This is a repository copy of *Hardware-in-the-loop simulation of magnetorheological dampers for vehicle suspension systems*.

White Rose Research Online URL for this paper:
http://eprints.whiterose.ac.uk/8860/

Article:

Hardware-in-the-loop simulation of magnetorheological dampers for vehicle suspension systems

D C Batterbee and **N D Sims***
Department of Mechanical Engineering, The University of Sheffield, Sheffield, UK

Abstract: Magnetorheological (MR) fluids provide an elegant means to enhance vibration control in primary vehicle suspensions. Such fluids can rapidly modify their flow characteristics in response to a magnetic field, so they can be used to create semi-active dampers. However, the behaviour of MR dampers is inherently non-linear and as a consequence, the choice of an effective control strategy remains an unresolved problem.

Previous research has developed a method to linearize the damper's force/velocity response, to allow implementation of classical control techniques. In the present study, this strategy is used to implement skyhook damping laws within primary automotive suspensions. To simulate the vehicle suspension, a two-degree-of-freedom quarter car model is used, which is excited by realistic road profiles. The controller performance is investigated experimentally using the hardware-in-the-loop-simulation (HILS) method. This experimental method is described in detail and its performance is validated against numerical simulations for a simplified problem.

The present authors demonstrate that feedback linearization can provide significant perform-ance enhancements in terms of passenger comfort, road holding, and suspension working space compared with other control strategies. Furthermore, feedback linearization is shown to desensitize the controller to uncertainties in the input excitation such as changes in severity of the road surface roughness.

Keywords: magnetorheological, HILS, feedback linearization, vehicle, suspension, control

1 INTRODUCTION

It is well known that semi-active damping devices can offer an attractive compromise between the simplicity of passive systems, and the cost of higher-performance fully active approaches [**1**]. Consequently, there has been a great deal of research to develop such dampers, along with suitable control strategies.

An elegant method of creating a semi-active damper is to use a smart fluid as the operating medium [**2**]. This fluid can rapidly modify its flow characteristics when subjected to an electric or magnetic field. In particular, magnetorheological (MR) fluids, which respond to magnetic fields, have seen widespread commercial success in recent years [**3**].

The configuration of an MR damper is shown schematically in Fig. 1. As the damper piston moves, the MR fluid is forced through an annular orifice (the 'MR valve'), which is exposed to a magnetic field generated by a coil. This leads to the formation of particle chains that increase the resistance to fluid flow, thus enabling the development of a controllable damping force. A typical force–velocity relationship for an MR damper under different magnetic fields is shown in Fig. 2. Various applications of MR dampers have been considered, such as the seismic control of bridges [**4**] or tall buildings [**5**], and suspension systems for vehicles [**6**], passenger seats [**7**], or washing machine drums [**8**].

One method that can be used to experimentally test such systems is the use of hardware-in-the-loop-simulation (HILS). This allows one aspect of the system to be physically tested, while the remainder of the structure is simulated in real time. For a vehicle suspension problem, the semi-active MR damper

* *Corresponding author: Department of Mechanical Engineering, University of Sheffield, Mappin Street, Sheffield S1 3JD, UK. email: n.sims@sheffield.ac.uk*
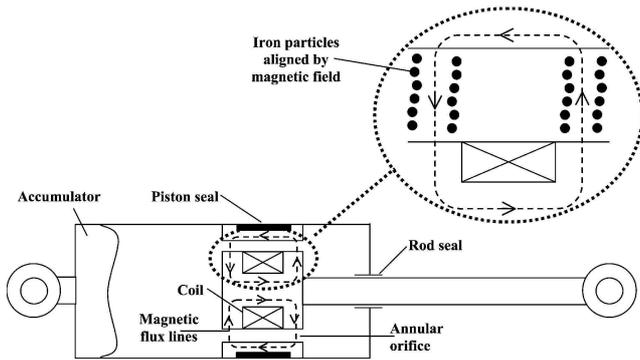
Fig. 1 MR damper design and operation
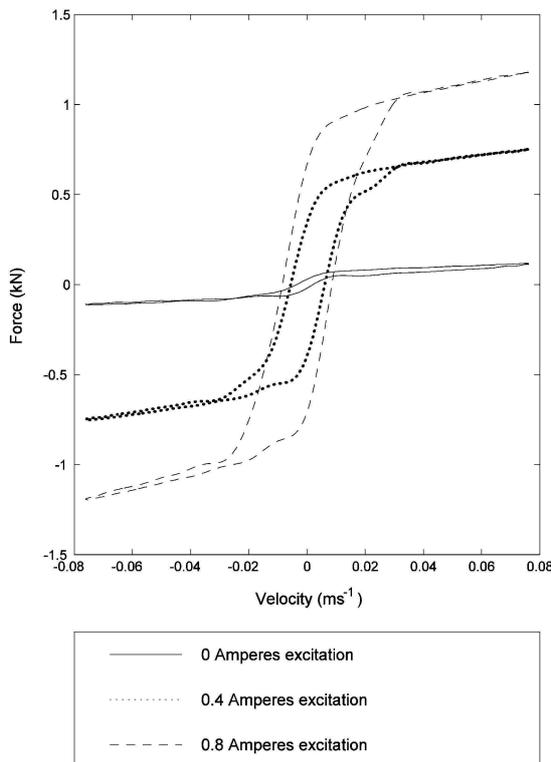
Fig. 2 Typical force/velocity response of an MR damper. Sinusoidal excitation – amplitude = 6 mm, frequency = 2 Hz

can be experimentally tested, while the dynamics of the vehicle are simulated. This enables the performance of the novel damper design to be characterized without building an actual suspension system. This technique was pioneered by Besinger, Cebon, and Cole in the 1990s, with particular emphasis on larger road vehicles [**9**, **10**]. However, this work did not consider the use of MR dampers, which pose additional problems owing to their highly non-linear behaviour [**11**]. More recently, researchers from the smart materials community have considered the use of HILS techniques for MR dampers [**12–16**],

but the complex behaviour of the dampers means that the choice of control strategy remains an unsolved problem.

Previous research by the present authors [**6**, **14**, **17–19**] has focussed on a control strategy that can enable the device to operate as a semi-active force generator, enabling the use of classical suspension control strategies. To date, the application of this approach has been investigated by HILS testing of single-degree-of-freedom (SDOF) structures [**14**]. In the present article, the work is extended to consider in detail the problem of automotive suspension systems, using a quarter-car model [**20**]. The paper is organized as follows: after introducing the theoretical approach with particular emphasis on controller design, the hardware and software configuration is described. This experimental method is then validated by comparing model and experimental data for a simplified problem. The experimental data for the suspension system problem are then presented, and performance comparisons are made between the different control strategies. Finally, some conclusions are drawn regarding the relative performance of different control systems, along with the suitability of HILS testing for this class of problem.

2 VEHICLE MODELLING AND CONTROL OBJECTIVES

It is well known that the ride characteristics of passenger vehicles can be characterized by considering the so-called 'quarter car' model [**20**]. Here, the system is reduced to a 2DOF lumped parameter model that considers the tyre stiffness and damping, unsprung mass, suspension stiffness and damping, and the sprung mass. This method has been widely used to investigate the performance of passive [**21**], semi-active [**9**], and fully active [**22**] suspension systems.

To excite the quarter car system, broadband random signals representative of typical roads can be used [**23**]. The road profiles can be generated using the following displacement power spectral density function $S(n)$

$$S(n) = Cn^{-w}\left(\frac{\text{m}^2}{\text{cycle/m}}\right) \qquad (1)$$

Here, n is the wavenumber (cycle/m), and C and w are fitting constants describing the severity of road roughness. The wavenumber n is given by f/V, where f is the vibration frequency and V is the vehicle speed. Consequently, for a given vehicle speed,

the inverse fast Fourier transform can be used to determine the road surface heights in the time domain [24]. In the present study, motorway and principal road excitations were generated with frequency content from 0 Hz to 20 Hz, and Table 1 shows the corresponding values of C, w, and V.

Under these excitation conditions, the performance of the suspension system can be characterized in terms of the following signals [20]:

(a) car body acceleration, which provides a measure of passenger comfort;
(b) wheel contact force, which provides a measure of road holding;
(c) suspension working space, which relates to the packaging space for the suspension system.

These signals can be presented in the time domain, frequency domain, or more compactly as root-mean-square (RMS) values. An effective semi-active suspension system control strategy should minimize all three signals. Before introducing some candidate control strategies, however, it is necessary to tackle the non-linearity of the MR damper, which makes application of control more complex.

2.1 Feedback linearization

MR dampers exhibit highly non-linear force/velocity characteristics, which makes the objective of achieving a desired force very difficult. To overcome this problem, work by the current authors and their colleagues has shown how the force/velocity response can be linearized [17]. The linearized MR damper can effectively emulate a viscous dashpot with a controllable damping coefficient. Thus the control problem is simplified to the determination of the linear damping rate that provides the desired force. This control strategy is known as feedback linearization, which is briefly summarized below.

The fundamental controller associated with feedback linearization is illustrated in Fig. 3. Here, feedback control is being used to implement a semi-active force generator. Through the appropriate selection of the feedforward gain G, and the feedback gain B, it can be shown that the actual damping force F becomes equal to the desired set-point damping force F_d [25]. Consequently, if the set-point force is
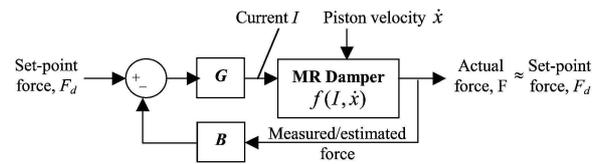
Fig. 3 Controller block diagram of the semi-active force generator

proportional to the piston velocity, then the MR damper response is linearized. For the present study, values of G equal to 0.001 A/N and B equal to 0.8 were found to provide a good response (further details regarding the choice of controller gain can be found in references [18] and [26]). For the values chosen, the performance is illustrated in Fig. 4, where the sinusoidal response of the MR damper has been linearized. Here the set-point force to the controller (Fig. 3) was

$$F_d = Dv \qquad (2)$$

where D is the set-point gain or the desired damping rate and v is the piston velocity. As shown, when $D = 6$ kNs/m the response becomes almost linear. Moreover, the actual damping rate correlates very well with the desired damping rate, thus demonstrating the controller's force tracking capability. The responses
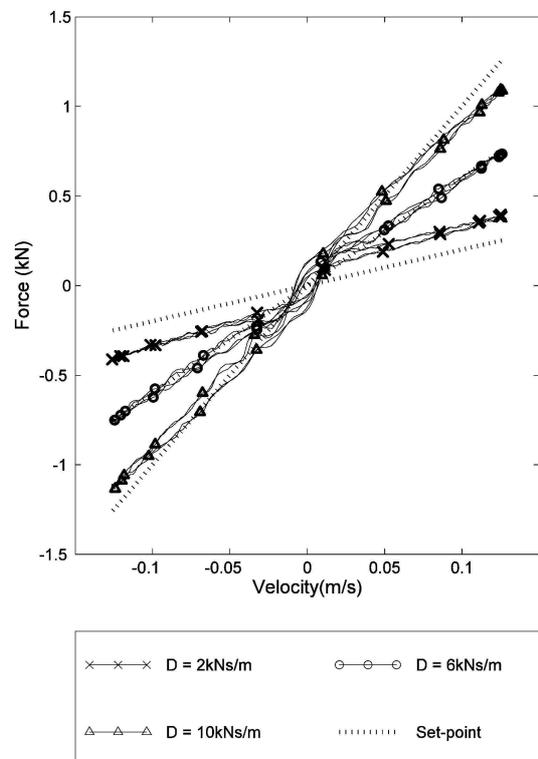
Fig. 4 Linearized sinusoidal force/velocity response. Amplitude = 5 mm, frequency = 4 Hz

Table 1 Road profile parameters

Profile	C (m$^{1/2}$ cycle$^{3/2}$)	w	V (miles/h)
Motorway	7×10^{-8}	2.5	70
Principal road	50×10^{-8}	2.5	60

for $D = 2$ kNs/m and $D = 10$ kNs/m represent the control limits of the device. When $D = 2$ kNs/m, the set-point damping force is lower than the minimum value that is governed by the viscosity of the MR fluid. Consequently, the current is set to zero amps, and the desired force is not achieved. It should be noted that the yield force effect that can be observed in this response is attributable to friction in the damper seals. For $D = 10$ kNs/m, the set-point force is accurately achieved between ± 0.06 m/s. Beyond ± 0.06 m/s, saturation occurs as the maximum yield stress in the fluid has been reached, i.e. the current is at its maximum value. Consequently, the actual force falls short of the set-point value.

In the above example, the set-point force is always a dissipative one, i.e. the direction of the desired force is always in the same direction as the actual force. However, in a real control system, the set-point damping force may require an energy input into the system. In this scenario, the force produced by the damper opposes the desired value, and the MR control current will be switched off in order to minimize the energy dissipated.

In summary, feedback linearization provides an excellent force tracking strategy for MR dampers. However, it is still necessary to choose an appropriate value of the desired force at each point in time, and so some possible approaches will now be described.

2.2 Vehicle suspension control strategies

Four different suspension control strategies were investigated in the present study.

2.2.1 Open-loop

To provide a performance benchmark for the controlled MR systems, an open-loop controller was investigated. Here, the feedback linearization procedure that was described in the previous section was not used. Instead, the current supplied to the MR damper was maintained at a constant level I_{OL}, where values between 0 and 0.2 A were investigated.

2.2.2 Linearized

As a more realistic benchmark, the MR damper was linearised using the controller that was discussed in section 2.1, so that the set-point force to the semi-active force generator (Fig. 3) was

$$F_d = D(\dot{x}_c - \dot{x}_w) \tag{3}$$

where $\dot{x}_c$ is the velocity of the car body, and $\dot{x}_w$ is the velocity of the wheel/axle assembly. This system is more representative of a conventional passive suspension with a viscous damper. The set-point

gain D was varied between 1 kNs/m and 5 kNs/m, which approximately corresponds to sprung mass damping ratios between 0.2 and 1.

2.2.3 Linearized modified skyhook control

Skyhook control is well known to provide optimal performance for SDOF vibration systems. Here, the damping force is proportional to the absolute velocity of the vibrating mass, so that

$$F_d = D_{sky}\dot{x}_c \tag{4}$$

This is known as linearized skyhook control, where D_{sky} is the skyhook set-point gain. For 2DOF systems such as the quarter car, pure skyhook control attenuates vibration at the natural frequency of the sprung mass, but has an adverse effect at the natural frequency of the wheel mass (wheel hop frequency). This has led to an alternative strategy known as modified skyhook control, which augments skyhook damping with body to wheel relative motion damping as an attempt to gain the advantages of both [9]. In the present study, the MR damper is used to achieve the modified skyhook damping force. This is known as linearized modified skyhook control, and with reference to Fig. 3, the set-point control force F_d is

$$F_d = D_{sky-m}[\alpha(\dot{x}_c - \dot{x}_w) + (1 - \alpha)\dot{x}_c] \tag{5}$$

Here, α is a weighting parameter between 0–1, and D_{sky-m} is the modified skyhook set-point gain. When $\alpha = 1$, the desired force corresponds to linear body to wheel relative motion damping (which is identical with the linearized system – equation (3)) and when $\alpha = 0$, the set-point force corresponds to pure skyhook control (equation (4)). It will be shown in section 5 that this set-point force can be accurately achieved within the dissipative control limits of the MR damper.

2.2.4 On/off modified skyhook control

On/off modified skyhook control involves switching the input current to a predetermined and constant level when the set-point force is a dissipative one

$$I = I_{max}: \quad [\alpha(\dot{x}_c - \dot{x}_w) + (1 - \alpha)\dot{x}_c](\dot{x}_c - \dot{x}_w)$$
$$> 0 - \text{energy dissipation required} \tag{6}$$

$$I = 0: \quad [\alpha(\dot{x}_c - \dot{x}_w) + (1 - \alpha)\dot{x}_c](\dot{x}_c - \dot{x}_w)$$
$$\leqslant 0 - \text{energy input required} \tag{7}$$

Here, the controller gain I_{max} dictates the current applied in the 'damper on' condition, and this was varied between 0.05 A and 0.2 A. Since no force feedback is required, the need to measure or estimate

the damping force is eliminated. On/off control therefore represents a major simplification over the linearised modified skyhook controller. However, the performance may suffer.

3 EXPERIMENTAL SET-UP

When certain aspects of the model have particularly complex behaviour, such as a semi-active damper, the gap between theory and practice can be bridged by performing hardware-in-the-loop simulations. In the present study, the HILS configuration shown in Fig. 5 was used. Here, the non-physical quarter car parameters are modelled in a real-time simulation. Using digital-to-analogue conversion, outputs from this simulation (damper displacement and control current) are used to excite the MR damper. Simultaneously, an analogue-to-digital converter provides the simulation with damping force data in order to complete the solution of the equations of motion. A photograph of the experimental facility is shown in Fig. 6.

With reference to Figs 5 and 6, a host PC running xPC target is used to both implement the damper control strategies, and model the non-physical system parameters. This model is then downloaded onto a target PC, which performs the real-time simulation by communicating to and from the hardware via a National Instruments data acquisition card. An Instron servohydraulic actuator and controller was used to excite a Carrera MagneShock MR damper, with a controlled displacement commanded by the target PC's quarter car simulation. To power the MR damper, a high performance Kepco BOP amplifier was used, providing high bandwidth dynamic current control. The actuator instrumentation included a built-in inductive displacement transducer, which was used for position feedback control of the servo-hydraulic actuator. Also, a dynamic load cell provided the force data for linearization of the MR damper, and simulation of the quarter car model.

At this stage, it is worth pausing to consider the practical issues concerned with implementing the various controllers within an actual vehicle. The sky-hook controllers described in section 2.2 require measurements of the absolute car body velocity, and the relative car body to wheel velocity. Such measurements can be difficult to obtain from displacement sensors, especially the absolute velocity due to the lack of an inertial reference. However, previous research has shown how these variables can be obtained by integrating accelerometer signals [27, 28]. For example, Simon and Ahmadian [28] implemented on/off skyhook control onboard a heavy truck. The authors used eight accelerometers in order to calculate the absolute car body and wheel velocities at each corner of the vehicle. With regards more specifically to feedback linearization, a means to measure the damping force is also required. This
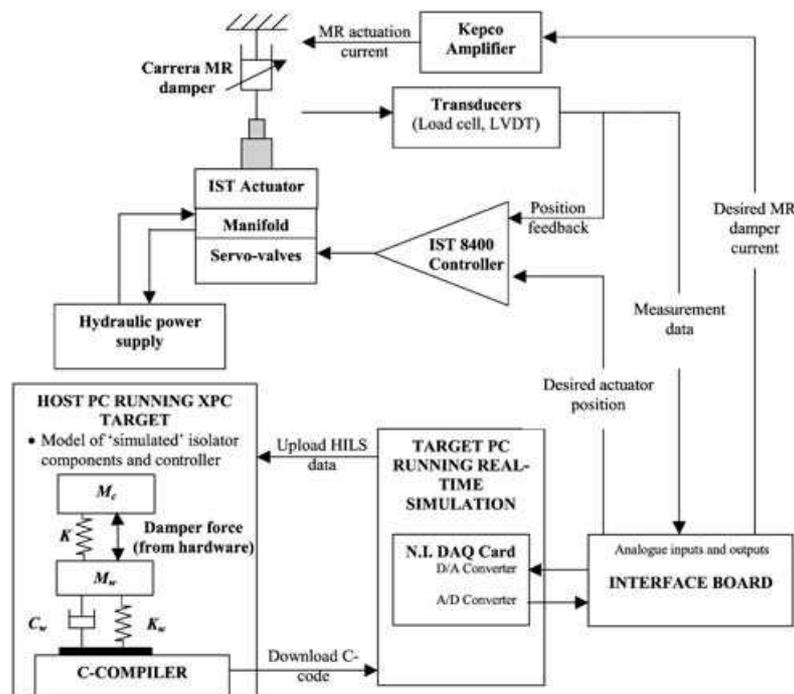
Fig. 5 Schematic diagram of the HILS experimental facility
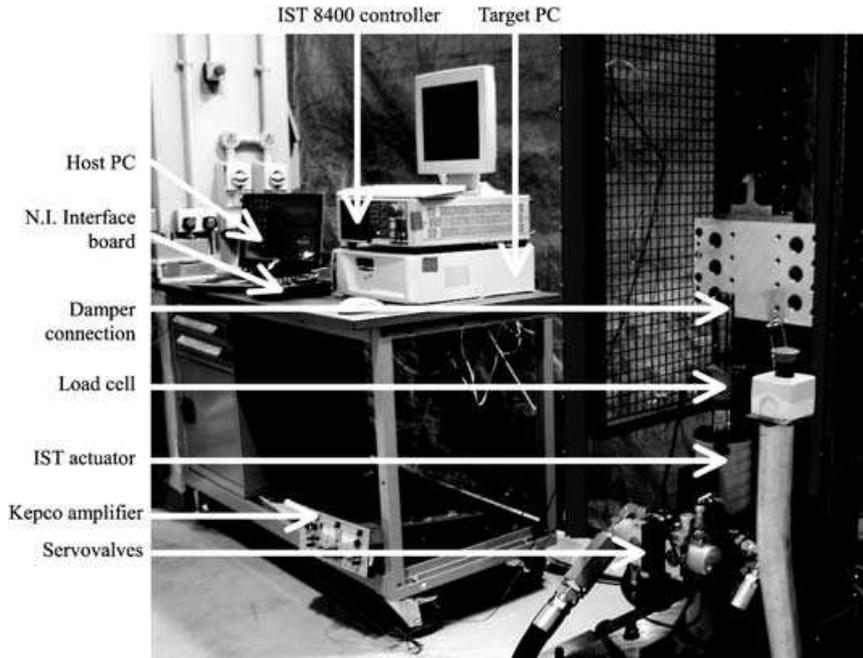
Fig. 6 Photograph of the HILS experimental facility (with no damper installed)

could be accomplished using a load cell at each corner of the vehicle, or the force could be derived from a state estimator used in conjunction with the accelerometer signals. Such considerations are outside the scope of the present research but would be an interesting topic for future research.

In the HILS experimental system, the velocity measurements are calculated in the 'virtual' loop and so sensors are not required. However, a complication arises owing to the presence of the actuator dynamics, which causes the actual damper displacement to lag behind the desired displacement. For the actuator in the current study, the phase delay was found to be 6 ms in the frequency range of interest [**14**]. This delay means that the 'simulated' velocity of the mass, which is used to compute the set-point skyhook force (and hence current), does not coincide with the force and displacement that is actually being measured. To correct for this, an additional time delay (6 ms in this case) must be incorporated into the controller. This is illustrated in Fig. 7 for a linearized skyhook controller, where the velocity of the mass has been delayed by 6 ms. Consequently, the velocity used to compute the set-point force is brought back in phase with the actual velocity.

Fig. 7 Skyhook control implementation with the HILS quarter car system

Fig. 8 A schematic diagram of the HILS system numerical model

The inclusion of the above delay compensates for the velocity lag in the controller, but there is still a 6 ms delay in the force signal received by the real-time simulation from the physical test rig. This will affect the accuracy of the HILS results, e.g. sprung mass velocity, and thus it is prudent to validate the experimental method, which is the subject of the next section.

4 HILS VALIDATION

Previous work [14] by the present authors used the HILS test facility to investigate a SDOF vibration isolator using an MR damper. A comprehensive model of the damper, HILS test rig, and control system was developed that allowed a detailed comparison between modelled and experimental behaviour. This work will now be summarized to demonstrate the validity of the HILS testing approach.

Using a previously validated model of the MR damper [29], along with a servohydraulic system model, a numerical simulation of the hardware-in-the-loop experiment was made possible. This will be referred to as the 'HILS simulation' and the corresponding numerical model is illustrated schematically in Fig. 8; by removing the model of the actuator, giving the 'ideal simulation', the effect of the actuator dynamics can be investigated.

Figure 9 compares the HILS experiment with the HILS simulation for a linearized skyhook controller. The results are shown in terms of the transmissibility estimate, where a broadband displacement excitation was used. For both skyhook gains, good correlation exists between the HILS simulation and the HILS experiment, thus validating the numerical model of the HILS testing method.

Fig. 9 Transmissibility estimates of the linearized sky-hook SDOF systems [14]

By subsequently removing the actuator dynamics from the numerical model a good indication of the performance of the real system will result. Moreover, the effect of the servohydraulic system dynamics on control system performance will be evident. The result is also shown in Fig. 9 as the 'ideal simulation'. It can be observed that the main effect of the actuator dynamics is to increase transmissibility thus degrading performance. This is particularly the case at higher frequencies (above 7–8 Hz), where the 6 ms delay results in a more

significant error in the force amplitude received by the simulation. Although this provides an inaccurate representation of the high-frequency response, it was previously shown that the relative performance between different control strategies remains largely unchanged [**14**]. The HILS approach therefore serves as an effective prototyping tool, as a good assessment of the relative controller performance can still be determined. Owing to the large similarities between the SDOF isolator and the 2DOF quarter car system, this result serves to validate the use of the HILS method in the present study.

5 EXPERIMENTAL RESULTS

The HILS testing technique can now be used with confidence to investigate the performance of the quarter car system, using the control strategies described in section 2.2. The non-physical system parameters used in this study are presented in Table 2, which were chosen to represent a small sized passenger car. For this vehicle configuration, the Carrera MR damper provided a zero-field damping rate ζ_{min} approximately equal to 0.56. To maximize the performance of a semi-active device, it is desirable for ζ_{min} to be small so that the energy dissipated is minimized when an energy input is required. A scaling factor of 0.36 was therefore applied to the measured damping force F in order to lower ζ_{min} to 0.2. In practice, this scaling could be achieved by modifying the damper's internal geometry.

To begin, Fig. 10 illustrates the effectiveness of the MR damper as a semi-active force generator. Here, the time history of the set point and actual damping forces is compared for the motorway excited linearized system. Clearly, the accuracy of the semi-active force generator is excellent, where the actual damping force tracks the commanded value very closely. This example serves to illustrate the usefulness of performing feedback linearization on MR dampers.

In Fig. 11, the power spectral density (PSD) responses of the linearized modified skyhook system are presented for the motorway excitation. Results
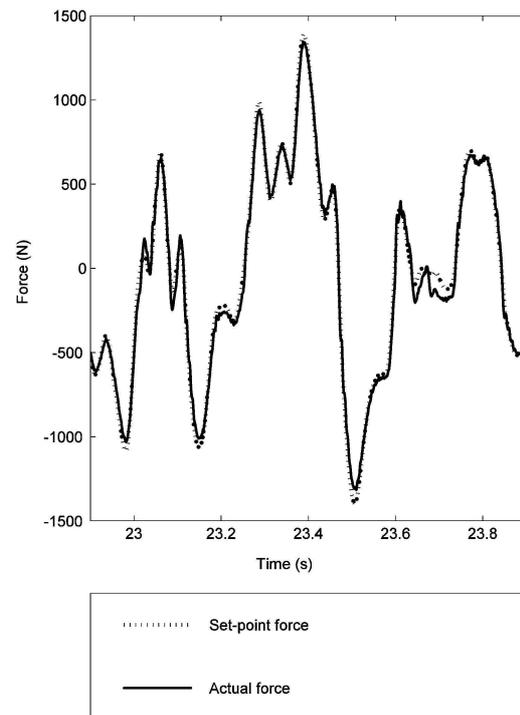
Fig. 10 Damping force–time history for the linearized quarter car systems. $D = 3$ kNs/m. Motorway excitation

are shown for $D_{sky\text{-}m} = 4$ kNs/m where α is varied between zero and one. With reference to Fig. 11(a), skyhook control ($\alpha = 0$) is most superior in terms of passenger comfort, where significantly lower PSD values are observed between 0 and 10 Hz. However, the disadvantage of pure skyhook control becomes apparent through observation of the wheel contact force prediction. As shown in Fig. 11(b), pure skyhook control minimizes the sprung mass resonant peak but the wheel hop vibrations become significantly larger, as evidenced by the increased wheel force variation in the 9 to 14 Hz range. Figure 11(b) thus illustrates the advantages of using a modified skyhook strategy ($0 < \alpha < 1$), where by augmenting the skyhook system with linear body to wheel relative motion damping, the unsprung mass vibrations are improved. However, this improvement is at the expense of the sprung mass vibrations thus the suspension designer must tune α until a desirable trade-off in performance is achieved.

For the linearized modified skyhook system, the desired force is not always dissipative, so it is interesting to investigate how effectively the MR damper can track the desired force. This is shown in Fig. 12, and the instants in time when an energy input is required are also indicated. During these instants, the set-point force is in the opposite

Table 2 Quarter car suspension parameters

Parameter	Symbol (unit)	Value
Mass of car body	M_c (kg)	275
Mass of wheel assembly	M_w (kg)	50
Suspension stiffness	K (N/m)	30 400
Tyre stiffness	K_w (N/m)	229 500
Tyre damping rate	C_w (Ns/m)	80
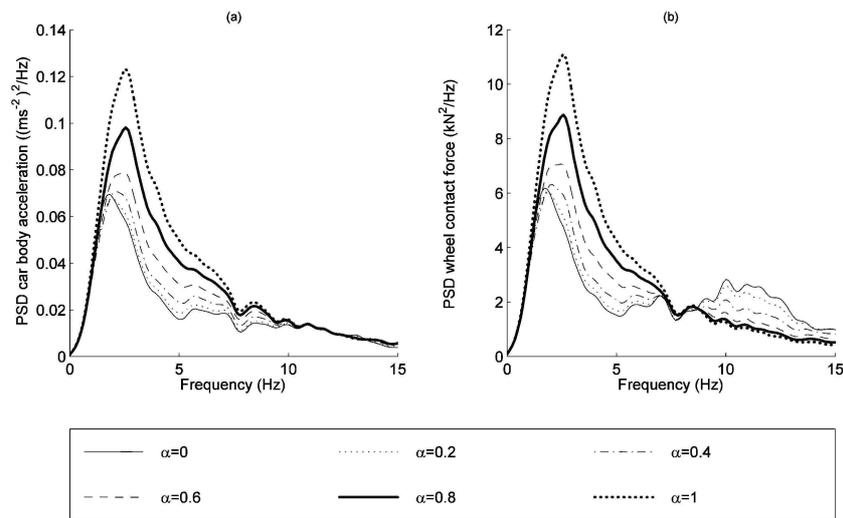
Fig. 11 Frequency response of the linearized modified skyhook system. $D_{\text{sky-m}} = 4$ kNs/m. Motorway excitation. (a) car body acceleration; (b) wheel contact force
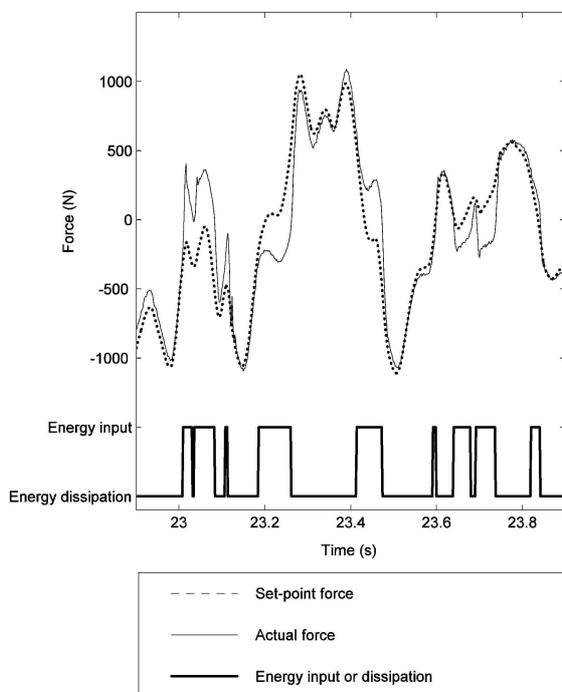
Fig. 12 Damping force-time history for the linearized modified skyhook quarter car system. $D_{\text{sky-m}} = 4$ kNs/m, $\alpha = 0.4$. Motorway excitation

direction to the actual force, and so – as expected – the performance of the semi-active force generator deteriorates. Nonetheless, when the desired force is a dissipative one, the force tracking accuracy is very good as before. Furthermore, it was found that an energy input was only required for 20 per cent of the entire HILS test. This suggests that the performance of the semi-active MR system is likely to approach that of a fully active system. In conclusion, the semi-

active force generator performs extremely well in the face of broadband random excitations. This force tracking strategy could equally be applied to achieve force demands from other controllers, such as sliding mode or optimal controllers.

The performance of the motorway excited on/off modified skyhook system is shown in Fig. 13. This is shown for $I_{\text{max}} = 0.15$ A where α is varied between zero and one. As with the linearized modified skyhook system, pure skyhook control ($\alpha = 0$) provides the most superior response in terms of passenger comfort (Fig. 13(a)). However, with reference to Fig. 13(b), the on/off system is unable to significantly suppress the wheel hop vibrations when α is increased. Although some improvement can be observed for $\alpha > 0$, an analysis of the area under the PSD curves illustrates that there is no improvement in the RMS wheel contact force. Thus it is concluded that pure skyhook control is more suitable than modified skyhook control, for an on/off system. This result is in agreement with the present authors' previous findings in a recent numerical study of a quarter car MR suspension [6].

It is difficult to find optimal controller parameters based directly upon the frequency response of the system. An alternative approach is to compare the RMS value of one performance indicator against another, as a function of a control parameter. This is known as a conflict diagram [9], and the optimal system will have its operating point closest to the origin where all of the performance indicators have been minimized.

Figure 14 shows the conflict diagram for the motorway excitation, where the RMS car body acceleration (Fig. 14(a)) and RMS wheel contact force
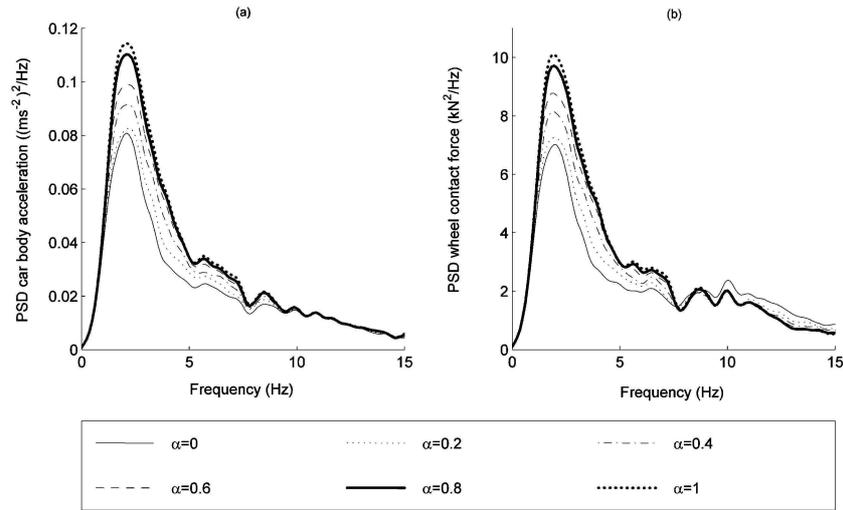
Fig. 13 Frequency response of the on/off modified skyhook system. $I_{max} = 0.15$ A. Motorway excitation. (a) car body acceleration; (b) wheel contact force
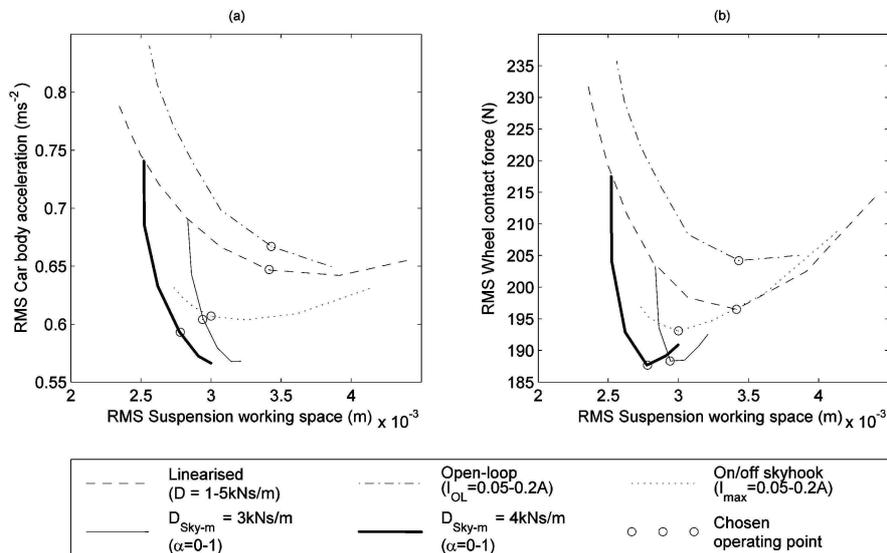
Fig. 14 Conflict diagrams for the motorway excitation. RMS suspension working space versus: (a) car body acceleration; (b) wheel contact force

(Fig. 14(b)) are plotted against the RMS suspension working space. In Fig. 14, the variable parameter for each control system is as follows:

(a) open-loop: I_{OL} is varied between 0.05 and 0.2 A;
(b) linearized: D is varied between 1 and 5 kNs/m;
(c) linearized modified skyhook: curves are plotted for $D_{sky-m} = 3$ kNs/m and 4 kNs/m, where α is varied between 0 and 1.
(d) on/off modified skyhook: as skyhook control is optimal for this system (see Fig. 13), $\alpha = 0$ and I_{max} is varied between 0.05 A and 0.2 A.

With reference to Fig. 14, the open-loop system clearly has the worst performance. This is owing to

the non-linear force/velocity characteristics, which creates a harsh response when the velocity changes direction. The linearized system, which better emulates a passive device, improves on this response but it is the skyhook-based controllers that provide the best performance. Moreover, the linearized modified skyhook system is superior to the on/off skyhook system, where lower levels of car body acceleration and wheel contact force can be achieved. Figure 14 also confirms that pure skyhook control ($\alpha = 0$) is optimal in terms of minimizing car body acceleration. Furthermore, the linearized skyhook system provides superior wheel contact force levels to the linearized 'passive' configuration.
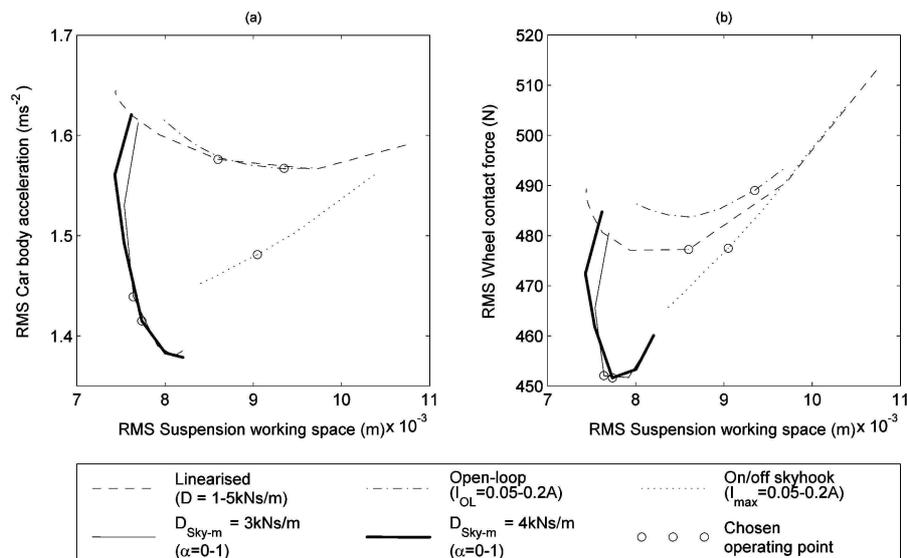
Fig. 15 Conflict diagrams for the principal road excitation. RMS suspension working space versus: (a) car body acceleration; (b) wheel contact force

Similar conclusions can be drawn from Fig. 15, which presents the conflict curves for the principal road excitation. However, a further advantage of linearized modified skyhook control arises via a comparison of Fig. 14 with Fig. 15. Except for the linearized modified skyhook system, the shape of the conflict curve changes with the input excitation. This causes the optimum controller gain to change and performance suffers, particularly for the on/off and open-loop strategies. This point is better explained with the following example. An operating point for each control system was chosen such that the wheel contact force is minimized on the motorway. These operating points are highlighted on Fig. 14 by the circular markers, and the corresponding control parameters are given in Table 3. The performance of the same controller configurations is then shown on Fig. 15 for the principal road excitation. Clearly, wheel contact force levels are no longer optimal, except for the linearized systems. As the main difference between the two road inputs is the excitation amplitude, these changes in the optimum

Table 3 Controller parameters for the optimized control systems

Control strategy	Controller gain	α
Linearized	$D = 2\,\text{kNs/m}$	–
Open-loop	$I = 0.075\,\text{A}$	–
MR linearized modified skyhook	$D_{\text{MRm}} = 4\,\text{kNs/m}$	0.4
On/off modified skyhook	$I_{\text{max}} = 0.125\,\text{A}$	0

controller gain are evidence of strong non-linearity in the on/off skyhook and open-loop systems. Thus it is apparent that feedback linearization has desensitized the otherwise non-linear MR damper to variations in the input excitation.

The latter result is summarized in Fig. 16, which shows the performance of the optimized controllers as a percentage improvement over the linearized system. As shown, linearized modified skyhook control is superior for all performance indicators and input excitations. For the motorway excitation, improvements in car body acceleration (CBA), wheel contact force (WCF), and suspension working space (SWS) are 8.3, 4.5, and 18.7 per cent respectively. The motorway excited on/off skyhook system also performs well where improvements are 6.2 per cent CBA, 1.7 per cent WCF, and 12.1 per cent SWS. However, when the input excitation changes, the on/off system performance is degraded and no improvement in wheel contact force and suspension working space is offered. On the other hand, the linearized modified skyhook system maintains superior performance, where improvements are 10.2 per cent CBA, 5.4 per cent WCF and 10 per cent SWS. It is also shown how the performance of the open-loop system is inferior to the linearized system for all but one of the performance indicators and excitation conditions. This indicates that the open-loop MR system is a poor benchmark for demonstrating the performance of a closed-loop MR system, since this still does not necessarily imply that the closed-loop behaviour is better than a passive system.

Fig. 16 Percentage performance improvements over the linearized system. Optimum controller parameters are given in Table 3

6 CONCLUSIONS

The current paper has described the performance assessment of semi-active suspension systems using hardware-in-the-loop simulation and a magnetorheological damper. Despite the dynamics of the servohydraulic actuation system, and the complex behaviour of the MR damper, the experimental method has been shown to enable a comprehensive comparison between different control strategies. Before drawing specific conclusions, it is worthwhile to compare this paper with previous contributions in the field.

The use of HILS testing for semi-active vehicle suspension was described in detail by Cebon and his colleagues [9, 10]. However, at that time MR dampers were relatively undeveloped and so these earlier studies did not investigate the control problems associated with them. More recently MR dampers have been used in HILS testing [12, 16], but to the current authors' knowledge none of these contributions accurately modelled the roadway excitation conditions, while considering the conflict diagram to interpret performance. Since MR dampers are particularly non-linear, their performance can be especially sensitive to the excitation. Consequently, this study has intentionally focused on two different, but physically realistic excitation conditions, unlike previous work. At the same time, the present study has included a novel technique to linearize the otherwise non-linear behaviour of the MR damper, thus enabling the use of classical semi-active control strategies.

With regards to the HILS testing method in general, it was shown that the effect of the servohydraulic

system dynamics is to degrade performance, particularly at higher frequencies. For a vehicle suspension, the wheel hop response may therefore be particularly inaccurate. Nonetheless, the relative performance between different control strategies should remain unchanged [14], which serves to validate the efficacy of the HILS method for controller prototyping.

The specific conclusions of this work are therefore as follows.

1. The open-loop control response is worse than the linearized 'passive' system in terms of all performance indicators. Therefore, this is a poor benchmark system for MR vibration control studies, since a semi-active performance better than the open-loop case is not necessarily better than a simple passive system.
2. Feedback linearization desensitises the controller to uncertainties in the input excitation. Unlike the equivalent on/off system, the performance remains optimal despite a change in severity of the road surface roughness.
3. Feedback linearization permits very accurate force tracking in the face of broadband random excitations. In the present study, this was demonstrated for skyhook-based controllers, although the control concept is equally applicable to other controller techniques such as optimal control.

ACKNOWLEDGEMENT

REFERENCES

1 **Karnopp, D., Crosby, M. J.,** and **Harwood, R. A.** Vibration control using semi-active force generators. *J. Engng Industry*, 1974, **96**, 619–626.

2 **Sims, N. D., Peel, D. J., Stanway, R., Johnson, A. R.,** and **Bullough, W. A.** The electrorheological long-stroke damper: A new modelling technique with experimental validation. *J. Sound Vibration*, 2000, **229**(2), 207–227.

3 **Carlson, J. D.** Magnetorheological fluids – engineering applications today and tomorrow. 2nd ECCOMAS Thematic Conference on *Smart structures and materials*, Lisbon, Portugal, 18–21 July 2005.

4 **Gordaninejad, F., Saiidi, M., Hansen, B. C., Ericksen, E. O.,** and **Chang, F.-K.** Magneto-rheological fluid dampers for control of bridges. *J. Intell. Mater. Systems Structs*, 2002, **13**(2–3), 167–180.

5 **Dyke, S. J., Spencer, B. F. Jr., Sain, M. K.,** and **Carlson, J. D.** Modelling and control of magneto-rheological dampers for seismic response reduction. *Smart Mater. Structs*, 1996, **5**, 565–575.

6 **Batterbee, D. C.** and **Sims, N. D.** Vibration isolation using smart fluid dampers: a benchmarking study. *Smart Structs Systems*, 2005, **1**(3), 235–256.

7 **McManus, S. J.** and **St Clair, K. A.** Evaluation of vibration and shock attenuation performance of a suspension seat with a semi-active magneto-rheological fluid damper. *J. Sound Vibration*, 2002, **253**(1), 313–327.

8 **Chrzan, M. J.** and **Carlson, J. D.** MR fluid sponge devices and their use in vibration control of washing machines. 8th SPIE Symposium on *Smart structures and materials: damping and isolation*, 2001, **4331**, 370–378.

9 **Cebon, D., Besinger, F. H.,** and **Cole, D. J.,** Control strategies for semi-active lorry suspensions. *Proc. Inst. Mech. Engrs, Part D: J. Automobile Engineering*, 1996, **210**, 161–178.

10 **Besinger, F. H., Cebon, D.,** and **Cole, D. J.,** Experimental investigation into the use of semi-active dampers on heavy lorries. Vehicle System Dynamics Proceedings of 12th IAVSD Symposium on *Dynamics of vehicles on roads*, 1991, pp. 57–71.

11 **Yi, F., Dyke, S. J., Caicedo, J. M.,** and **Carlson, J. D.** Experimental verification of multi-input seismic control strategies for smart dampers. *J. Engng Mech.*, 2001, **127**(11), 1152–1164.

12 **Lee, H.-S.** and **Choi, S.-B.** Control and response characteristics of a magneto-rheological fluid damper for passenger vehicles. *J. Intell. Mater. Systems Structs*, 2000, **11**(1), 80–87.

13 **Choi, S.-B.** and **Han, Y.-M.** MR seat suspension for vibration control of a commercial vehicle. *Int. J. Veh. Des.*, 2003, **31**(2), 202–215.

14 **Batterbee, D. C., Sims, N. D.,** and **Plummer, A.** Hardware-in-the-loop-simulation of a vibration isolator incorporating magnetorheological fluid damping. 2nd ECCOMAS Thematic Conference on *Smart structures and materials*, Lisbon, Portugal, 2005.

15 **Choi, S.-B., Song, H. J., Lee, H. H., Lim, S. C., Kim, J. H.,** and **Choi, H. J.** Vibration control of a passenger vehicle featuring magnetorheological engine mounts. *Int. J. Veh. Des.*, 2003, **33**(1–3), 2–16.

16 **Lam, A. H. F.** and **Liao, W. H.** Semi-active control of automotive suspension systems with magneto-rheological dampers. *Int. J. Veh. Des.*, 2003, **33**(1–3), 50–75.

17 **Sims, N. D., Peel, D. J., Stanway, R., Bullough, W. A.,** and **Johnson, A. R.** Controllable viscous damping: an experimental study of an electrorheological long stroke damper under proportional feedback control. *Smart Materials Structs*, 1999, **8**, 601–605.

18 **Sims, N. D., Stanway, R., Peel, D. J., Bullough, W. A.,** and **Johnson, A. R.** Smart fluid damping: shaping the force/velocity response through feedback control. *J. Intell. Mater. Systems Structures*, 2000, **11**, 945–949.

19 **Sims, N. D.** and **Stanway, R.** Semi-active vehicle suspension using smart fluid dampers: a modelling and control study. *Int. J. Veh. Des.*, 2003, **33**(1–3), 76–102.

20 **Crolla, D. A.** Vehicle dynamics: theory into practice. *Proc. Inst. Mech. Engrs, Part D: J. Automobile Engineering*, 1996, **210**, 83–94.

21 **Sharp, R. S.** and **Hassan, S. A.** Evaluation of passive automotive suspension systems with variable stiffness and damping parameters. *Veh. System Dynamics*, 1986, **15**(6), 335–350.

22 **Wilson, D. A., Sharp, R. S.,** and **Hassan, S. A.** The application of linear optimal control theory to the design of active automotive suspension. *Veh. System Dynamics*, 1986, **15**, 105–118.

23 **Robson, J. D.** Road surface description and vehicle response. *Int. J. Veh. Des.*, 1979, **1**(1), 25–35.

24 **Cebon, D.** and **Newland, D. E.** The artificial generation of road surface topography by the inverse FFT method. Proceedings of the 8th IAVSD Symposium on the *Dynamics of vehicles on roads and railway tracks*, Cambridge, Massachussets, Swets and Zeitlinger, 1994, pp. 29–42.

25 **Sims, N. D., Stanway, R.,** and **Beck, S. B. M.** Proportional feedback control of an electro-theological vibration damper. *J. Intell. Material Systems Structs*, 1997, **8**(5), 426–433.

26 **Sims, N. D.** Limit cycle behaviour of smart fluid dampers under closed-loop control. *J. Vibr. Acoustics*, 2006, **128**, 413–428.

27 **Ahmadian, M.** and **Gravatt, J.** A comparative analysis of passive twin tube and skyhook MRF dampers for motorcycle front suspensions. *Smart structures and materials 2004 – damping and isolation*, pp. 238–249 (International Society for Optical Engineering, Bellingham).

28 **Simon, D.** and **Ahmadian, M.** Vehicle evaluation of the performance of magnetorheological dampers for heavy truck suspensions. *J. Vibr. Acoustics*, 2001, **123**, 365–375.

29 **Sims, N. D., Holmes, N. J.,** and **Stanway, R.** A unified modelling and model updating procedure for electrorheological and magnetorheological dampers. *Smart Mater. Structs*, 2004, **13**, 100–121.

APPENDIX

Notation

B	feedback gain required for linearization
C	road roughness constant ($m^{1/2}$ cycle$^{3/2}$)
C_w	damping constant of the tyre (Ns/m)
D	set-point gain for the linearized system (Ns/m)
D_{sky}	set-point gain for the linearized skyhook system (Ns/m)
$D_{sky\text{-}m}$	set-point gain for the linearized modified skyhook system (Ns/m)
f	frequency (Hz)
F	actual damping force (N)
F_d	set-point or desired damping force (N)
G	feedforward gain required for linearization (A/N)
I	current supplied to the MR damper (A)
I_{max}	switching current for on/off skyhook control (A)
I_{OL}	constant current supplied to the open-loop system (A)
K	stiffness of the primary suspension (N/m)
K_w	stiffness of the tyre (N/m)
M	mass of the single-degree-of-freedom isolator (kg)
M_c	mass of the car body (sprung mass) (kg)
M_w	mass of the wheel/axle assembly (unsprung mass) (kg)
n	wavenumber (cycle/m)
S	power spectral density function of the road surface (m^3/cycle)
v	piston velocity (m/s)
V	vehicle speed (mile/h)
w	road roughness exponent
x_c	displacement of the car body (m)
x_r	displacement of the road input (m)
x_w	displacement of the wheel/axle assembly (m)
α	weighting parameter for the modified skyhook systems
ζ_{min}	zero-field damping rate of the MR damper
$\cdot$	over-dot represents differentiation with respect to time